

# The total mass of the atmosphere

Kevin E. Trenberth and Christian J. Guillemot

National Center for Atmospheric Research, Boulder, Colorado

**Abstract.** Accurate but approximate formulae for determining the mass of the atmosphere in terms of the surface pressure  $p_s$  are derived and applied to globally analyzed data from the European Centre for Medium-Range Weather Forecasts (ECMWF) for 1985 through 1993. The formulae take into account effects of the shape of the Earth and variations in gravity with latitude and height. Variations in total mass occur because of changes in the water vapor loading of the atmosphere. Independent computations are made of the surface pressure due to water vapor  $p_w$ , which is proportional to the precipitable water, using the ECMWF analyses of specific humidity. Spurious trends in both the mass of dry air and the atmospheric moisture are found to arise from changes in the analysis system at ECMWF, confounding attempts to seek real trends associated with climate change. For the recent 4-year period 1990 to 1993 the mean annual  $p_s$  was 984.76 mbar with a maximum in July of 984.98 mbar and a minimum in December of 984.61 mbar which correspond to a total mean mass of the atmosphere of  $5.1441 \times 10^{18}$  kg with a range of  $1.93 \times 10^{15}$  kg throughout the year associated with changes in water vapor in the atmosphere. The global mean  $p_w$  for 1985–1993 is 2.58 mbar, but values are 5 to 10% lower after mid-1992. Using the Special Sensor Microwave Imager data to make adjustments, the best estimate of the annual global  $p_w$  is 2.4 mbar, corresponding to  $\sim 2.5$  cm of precipitable water. The total atmospheric moisture as given by  $p_w$  varies with an annual cycle range of 0.36 mbar, a maximum in July, and a minimum in December. Thus the mean mass of water vapor is  $1.25 \times 10^{16}$  kg and the dry air mass is  $5.132 \times 10^{18}$  kg, corresponding to a mean surface pressure of 982.4 mbar. Overall uncertainties are  $\sim 0.1$  mbar or  $0.5 \times 10^{15}$  kg in total mass and about double those values for atmospheric moisture content. As well as the global means, hemispheric mean values and meridional profiles of  $p_s$  and  $p_w$  are presented for the mean annual cycle and as latitude-time series to show the interannual and longer-term variability.

## 1. Introduction

The mass of the atmosphere is a fundamental quantity for all atmospheric sciences and efforts to determine what it is have a long history that has involved many distinguished names in science. The exact value has become of increasing interest in recent times because of the attention being given to trace constituents in the atmosphere and their sources and sinks and budgets. As well as the intrinsic importance of trace constituents in atmospheric chemistry, changing concentrations of the radiatively active trace constituents, in particular, have a direct effect on climate. The trace constituents are typically measured as a mixing ratio in parts per million by volume or mass, or some other similar unit, so that the total mass of the atmosphere is needed to determine the absolute amounts.

A comprehensive review of previous estimates of global, northern hemisphere (NH) and southern hemisphere (SH) sea level pressures, surface pressures, and the total mass of the atmosphere was given by *Trenberth* [1981]. The purpose

of this paper is to update these values and acknowledge subsequent correspondence which pointed out some additional historical work that is of interest and the desirability of some further small corrections to the method. In addition, revised data sets allow us to provide a new estimate of the mass of the atmosphere and to further examine trends in the water vapor component of the total mass.

As noted by *Trenberth* [1981], it is the total mass of dry air in the atmosphere that is almost conserved as sources and sinks, such as outgassing in volcanoes, and losses to space are very small. However, the total mass of the atmosphere includes the trace constituents and water vapor, and as the latter varies significantly with the annual cycle, so too does the total atmospheric mass. Accordingly, there are two sources of information on the mean annual cycle of the total mass. One is from measurements of surface pressure over the globe, and the other is from measurements of water vapor in the atmosphere. In both cases, detailed knowledge of the surface topographic height is important and has a major influence on results, and revised estimates of the mountain heights have provided one source of change in the total mass estimates. Effectively there is an apparent exchange arising from whether part of the volume above sea level is occupied by solid earth or atmosphere. *Trenberth*

Copyright 1994 by the American Geophysical Union.

Paper number 94JD02043.  
0148-0227/94/94JD-02043\$05.00

*et al.* [1987] used a new topographic data set as well as new global analyses from the European Centre for Medium-Range Weather Forecasts (ECMWF) to revise the estimates of the total atmospheric mass. In addition, they exploited the two methods of estimating the annual cycle and were able to show that the global analyses indeed conserved dry air mass very closely and that there was excellent agreement between the annual cycle in total mass obtained both from direct estimates of the atmospheric moisture contribution and from the surface pressure. However, interannual variations (such as from the El Niño phenomenon) and long-term trends (such as might be expected in association with global warming and climate change caused by increased greenhouse gases in the atmosphere) were in the noise level of the data.

*Trenberth* [1981] outlined in detail the method of computing the total mass, given the surface pressure, and incorporated adjustments due to the shape of the Earth and variations due to gravity both with height and with latitude. In practice, in meteorology, the gravity variations are made transparent by making use of geopotential height, rather than geometric height, although the mass volume integral is in terms of geometric height. It has been pointed out by K. Bernhardt (Die Humboldt-Universität zu Berlin, through correspondence in 1988) that a further small correction (0.2%) is needed arising from differences between geopotential and geometric height and the variations of gravity with height that were not included earlier. *Bernhardt* [1991a] has also discussed this correction and its effects on the total mass and has given further estimates of how much the mass of the atmosphere should change due to increases in CO<sub>2</sub> [*Bernhardt*, 1991b]. Some other minor corrections are also desirable. Accordingly, we go over the method of computing the total mass below.

## 2. Historical Notes

*Trenberth* [1981] reviewed historical estimates of the mass of the atmosphere, sea level, and surface pressures. The first global mean sea level pressure maps were given by *Buchan* [1869]. From these *Ekholm* [1902] made an estimate of the mass of the atmosphere of  $5.16 \times 10^{18}$  kg that was widely quoted for many years. The fidelity of these first pressure charts, in retrospect, was remarkable. Apparently, the first estimate of the mass of the atmosphere was made shortly after the invention of the barometer about 1654, as reported by *Pascal* [1663] (Dave Fultz (University of Chicago) has brought to my attention these historical estimates of note and has documented them in a brief article [D. Fultz, unpublished article, 1990]). An estimate of mean surface pressure of 987.5 mbar is fortuitously close to modern estimates, but Pascal's estimate of the mass of the atmosphere of  $4.055 \times 10^{18}$  kg was well astray owing to a substantial underestimate of the size of the Earth. Much later, *Ferrel* [1877] used *Buchan*'s map to produce zonal mean sea level pressures every 5° of latitude which formed the basis for another estimate of the mass of the atmosphere by *Abbe* [1899], although his calculation seems to contain an error (D. Fultz, 1990). In fact, this map was apparently the primary basis for all estimates of the mass of the atmosphere up until the 1940s [see *Trenberth*, 1981].

## 3. Mass of the Atmosphere

The mass of the atmosphere  $m$  is given by

$$m = \int_{r_0}^{\infty} \int_0^{2\pi} \int_{-\pi/2}^{\pi/2} \rho r^2 \cos \phi \, d\phi \, d\lambda \, dz \quad (1)$$

where  $\rho = \rho(\lambda, \phi, r)$  is the density of air at longitude  $\lambda$ , latitude  $\phi$ , and  $r$  is the distance from the center of the Earth, where  $r = r_0$  at the surface of the Earth. A good approximation to the surface of the Earth is that of an ellipsoid where

$$r_0^2 = a^2 (1 - 2\alpha \sin^2 \phi) \quad (2)$$

where  $a$  is the equatorial radius ( $= 6378388$  m) and  $\alpha = (a^2 - b^2) / 2a^2 = 0.00336$  is closely related to the "flattening" and  $b$  is the polar radius ( $= 6356912$  m). Thus

$$r^2 = (a + z)^2 (1 - 2\alpha \sin^2 \phi) \quad (3)$$

where  $z$  is the height above the Earth's surface and

$$dr = (1 - 2\alpha \sin^2 \phi)^{\frac{1}{2}} dz.$$

By assuming that  $\rho = \rho_1(r) \rho_2(\lambda, \phi)$ , then

$$m = \int_0^{\infty} \int_{-\pi/2}^{\pi/2} \left[ \int_0^{2\pi} \rho_1(z) (a + z)^2 dz \right] \rho_2(\lambda, \phi) (1 - 2\alpha \sin^2 \phi)^{\frac{3}{2}} \cos \phi \, d\phi \, d\lambda \quad (4)$$

The main difficulty in evaluating (4) concerns the integral with respect to  $z$  and how to relate it to the measurements of surface pressure  $p_s$ , where

$$p_s = \int_0^{\infty} \rho_1(z) g(z) dz \quad (5)$$

and  $g$ , gravity, is a function of both height and latitude.

Also, it is necessary to recognize that all free atmospheric measurements are relative to geopotential not geometric height. At the surface of the Earth the latitude variations of gravity  $g$  in meters per second squared are given by

$$g_0(\phi) = 9.80616 (1 - 0.0026373 \cos 2\phi + 5.9 \times 10^{-6} \cos^2 2\phi). \quad (6)$$

This gives  $g_0 = 9.80616$  at 45° latitude, whereas all barometers and meteorological observations are standardized to  $g_0 = 9.80665$  m s<sup>-2</sup> at 45° latitude (an older value) and it is therefore necessary to use this number in place of the correct value in computing mass. In the vertical a sufficiently accurate approximation is

$$g = g_0 \frac{r_0^2}{r^2} = g_0 \frac{a^2}{(a + z)^2}. \quad (7)$$

Geopotential height  $Z$  is defined as

$$g_c Z = \int_0^z g dz$$

where  $g_c$  is a constant value of gravity, and up until about 1990 this was taken as  $g_c = 9.8$  m s<sup>-2</sup>, but in recent years there has been a transition to  $g_c = 9.80665$  m s<sup>-2</sup> =  $g_0$ . [Different countries have implemented the changeover at different times; in the United States the change was implemented on October 1, 1993.] Accordingly

$$g_c Z = g_0 \frac{az}{(a + z)} \quad (8)$$

and the hydrostatic relation can be written as

$$dp = -\rho g dz = -\rho g_c dZ. \quad (9)$$

The difference between  $g_c$  and  $g_0$  can be carried in this analysis, but as it ultimately drops out, it will be ignored.

To simplify (4), we temporarily assume an isothermal atmosphere of temperature  $T_0$ , so that

$$\rho_1(Z) = \rho_0 e^{-Z/H}$$

where  $H = \frac{RT_0}{g_c}$ . Then

$$\int_0^\infty \rho_1(z)(a+z)^2 dz = \int_0^{Z_t} \rho_0 e^{-Z/H} \frac{a^6}{(a-Z)^4} dZ \quad (10)$$

using (8) and where  $Z_t$  represents a practical top of the atmosphere. (This is done to avoid problems associated with the fact that as  $z \rightarrow \infty$ ,  $Z \rightarrow a$ , so the density is not zero, but the denominator  $\rightarrow 0$ . In practice, the approximations given above for gravity and geopotential break down above about 600 km altitude [Letestu, 1966].) Integrating by parts and recognizing that  $H/a$  is small ( $\sim 1.1 \times 10^{-3}$ ), to order  $(H/a)^3$

$$\int_0^\infty \rho_1(z)(a+z)^2 dz = a^2 \left( 1 + \frac{4H}{a} + 20 \left( \frac{H}{a} \right)^2 + O \left( \frac{H}{a} \right)^3 \right) \int_0^\infty \rho_1 dZ. \quad (11)$$

We can now remove our temporary assumption about the isothermal atmosphere, and because  $H/a$  is small, to a good approximation using (9)

$$\int_0^\infty \rho_1(z)(a+z)^2 dz \approx a^2 \left( 1 + \frac{4H}{a} \right) \int_{p_s}^0 \frac{dp}{g_0(\phi)}$$

so that

$$m = 2\pi a^2 \left( 1 + \frac{4H}{a} \right) \int_{-\pi/2}^{\pi/2} \frac{p_s(\phi)}{g_0(\phi)} (1 - 2\alpha \sin^2 \phi)^{\frac{3}{2}} \cos \phi d\phi \quad (12)$$

where  $p_s(\phi)$  is the zonal mean surface pressure. The  $g_0(\phi)$  is necessary in the denominator rather than  $g_c$  to properly convert values into mass accounting for the local values of gravity.

By making use of the fact that variations in surface pressure are mostly relatively small compared with the mean surface pressure, we can evaluate the contributions from the shape of the Earth and  $g(\phi)$ . The  $(1 + 4H/a)$  factor is 1.0044. Assuming  $p_s$  and  $g$  are constant with latitude, the  $\int_{-\pi/2}^{\pi/2} (1 - 2\alpha \sin^2 \phi)^{3/2} \cos \phi d\phi$  factor comes to 0.9966. Gravity varies relative to the standard value at  $45^\circ$  by factors of up to  $1 \pm 0.0026$  and modifies the global mean hardly at all, so that the ratio of the total integral to that without the shape and gravity factors (i.e., the global mean  $p_s$ ) is 0.9976. This number is robust using values of  $p_s$  in all months of the year. Thus when all three factors are combined, there is a certain amount of cancelation, so that

$$m = \frac{2\pi a^2 f}{g_0} \int_{-\pi/2}^{\pi/2} p_s(\phi) \cos \phi d\phi, \quad (13)$$

where  $f = 1.0020$  is the effect of the other three factors. In numerical terms

$$m = 5.22371 \times 10^{15} \bar{p}_s \quad (14)$$

where  $\bar{p}_s$  is the global mean areally weighted surface pressure in millibars and  $m$  is in kilograms.

#### 4. Data

The data used, as by *Trenberth et al.* [1987], are the global analyses from the European Centre for Medium-Range

Weather Forecasts (ECMWF) [Trenberth and Olson, 1988; Trenberth, 1992]. However, the data set differs in that it has 14 levels (15 beginning January 1992), instead of 7 in the vertical, is uninitialized, and is 4 times per day (instead of twice daily). The latter is an important advantage regionally because it allows the semidiurnal tide to be resolved. Here we use recent data from 1985 through 1993.

Methods for evaluating  $p_s$  were described by *Trenberth* [1981] who notes that it is necessary to transform the geometric height of the surface topography into a geopotential height for computing  $p_s$ . The method is also given by *Trenberth et al.* [1987] and *Trenberth* [1992] and it is important to note that the  $p_s$  was recomputed using the actual surface topography rather than using the archived ECMWF values which correspond to a spectral "envelope" orography. The latter is an enhanced orography which places the Earth's surface at surface pressures up to 100 mbar or more lower in value [Trenberth, 1992]. For 1985 to 1991 the global mean  $p_s$  from ECMWF was  $\sim 5$  mbar lower than we have computed. Justification of the enhanced topographic heights is made on the grounds that the free atmosphere does not dynamically connect with air in valleys. Also, the ECMWF representation is spectral, so that the surface has extensive ripples over the ocean, arising from Gibbs phenomena (ringing).

It seems that the greatest uncertainty in  $\bar{p}_s$  has been the height of the surface of the Earth, and revised topography was the main factor contributing to the revised estimate in *Trenberth et al.* [1987] versus *Trenberth* [1981]. In the work of *Trenberth* [1981] the global mean topographic height was 234.9 m versus the revised value of 237.33 m from the  $1/6^\circ$  latitude-longitude resolution topography prepared by the U.S. Navy Fleet Numerical Oceanography Center in *Trenberth et al.* [1987]. Regional differences were even larger, for instance the difference was +8.6 m for the NH. The topographical data set used in the most recent estimate is identical to that in the *Trenberth et al.* [1987] data set; however, the new data sets are at the higher resolution of T42 (triangular truncation in spherical harmonics at wave number 42) versus R15 (rhomboidal truncation at wave 15) earlier. As a result, there is a slight adjustment in the mean topographical values of 283.42, 191.32, and 237.37 m for the NH, SH, and the globe, respectively.

The surface pressure due to water vapor  $p_w$  is computed from the analyzed specific humidity fields

$$p_w = \int_0^{p_s} q dp = g_0 w \quad (15)$$

where  $w$  is the precipitable water. In this paper we reproduced the results of *Trenberth et al.* [1987] for 1985, but the new values are slightly lower because of the differences in vertical integral evaluation. Here we use 14 levels of data (versus 7 in the work of *Trenberth et al.* [1987]) and even though the additional levels are all in the upper troposphere, there is a decrease in  $p_w$  of 0.03 mbar (or 0.3 mm in  $w$ ). The addition of a 925-mbar level to the archive in January 1992 helps define the low-level moisture and contributes slightly to lower values (globally of 0.016 mb). Vertically integrating by interpolating relative humidity to 50 mbar-layers (instead of using specific humidity) would further decrease  $p_w$  by 0.04 mbar (or 0.4 mm in  $w$ ). A small change in the assigned thickness of the boundary layer (from 100 to 75 mbar) was implemented. These differences are systematic and do not influence changes with time.

## 5. Global Mass and Mean Annual Cycle

From *Trenberth et al.* [1987], estimates of  $\bar{p}_s$  were 984.43, 981.9, and 2.5 mbar corresponding to the mean total mass of the atmosphere, the mass of dry air, and the mean mass of water vapor. New values from our latest calculations for 1985-1993 are 984.70, 982.12, and 2.58 mbar (Figure. 1). The latter corresponds to 2.63 cm of precipitable water and is more uncertain for reasons discussed by *Trenberth et al.* and as will be seen later. These mean values are removed from the data to show the mean annual cycle of the fields in Figure 2.

Water vapor is a variable constituent, so that both the water vapor contribution and the total mass vary with an annual cycle of 0.37-mbar range and a maximum in July in  $p_w$  of 2.77 mbar and a minimum in December of 2.41 mbar (see also Figures 1 and 2). As the average temperature in the NH is larger than in the SH, its water-holding capacity is also larger, and even though the mean relative humidity

is generally less latitude by latitude (the exception being Antarctica), the moisture content is indeed greater in the NH [*Trenberth*, 1981]. Further, because of the larger annual cycle in temperature in the NH associated with the greater land mass, which is reflected in moisture-holding capacity and actual moisture itself, the maximum in water vapor and thus in total mass occurs in July [*Trenberth*, 1981].

Accordingly, for 1985-1993 from (14) the mass of the atmosphere varies by  $\pm 0.95 \times 10^{15}$  kg throughout the year with a mean value of  $5.1438 \times 10^{18}$  kg corresponding to  $1.35 \times 10^{16}$  kg of water vapor and  $5.1303 \times 10^{18}$  kg of dry air. The latter is 0.15% larger than values by *Trenberth et al.* [1987].

Figure 1 presents the hemispheric and global means of  $p_s$  and  $p_w$  and some interannual and longer-term variability is evident. This will be addressed in section 6. Figure 2 shows the hemispheric and global means together with their difference  $p_d = p_s - p_w$ , where  $p_d$  is the dry air mass. The global mean of the dry air mass should be constant and the

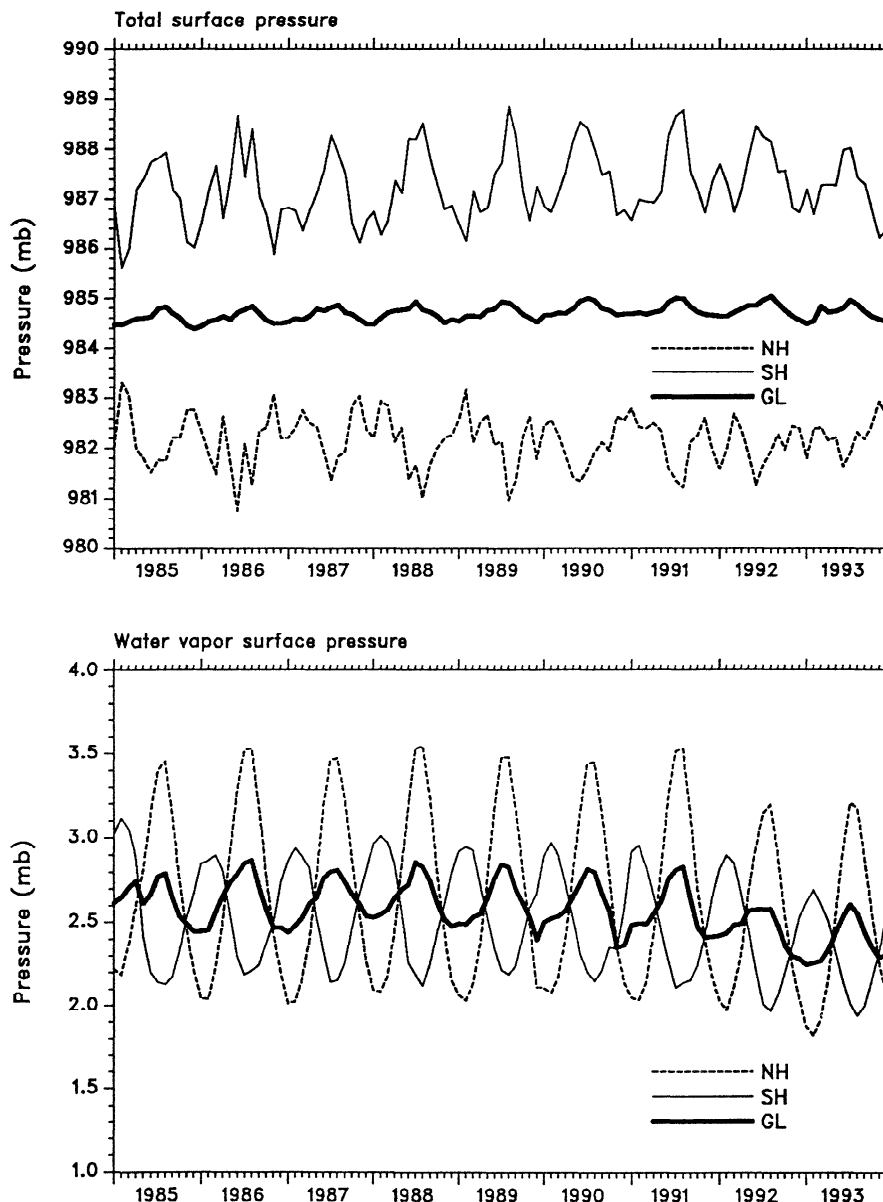


**Figure 1.** Times series plots of the hemispheric and global mean (top)  $p_s$  and (bottom)  $p_w$  for 1985 to 1993 in mbar.

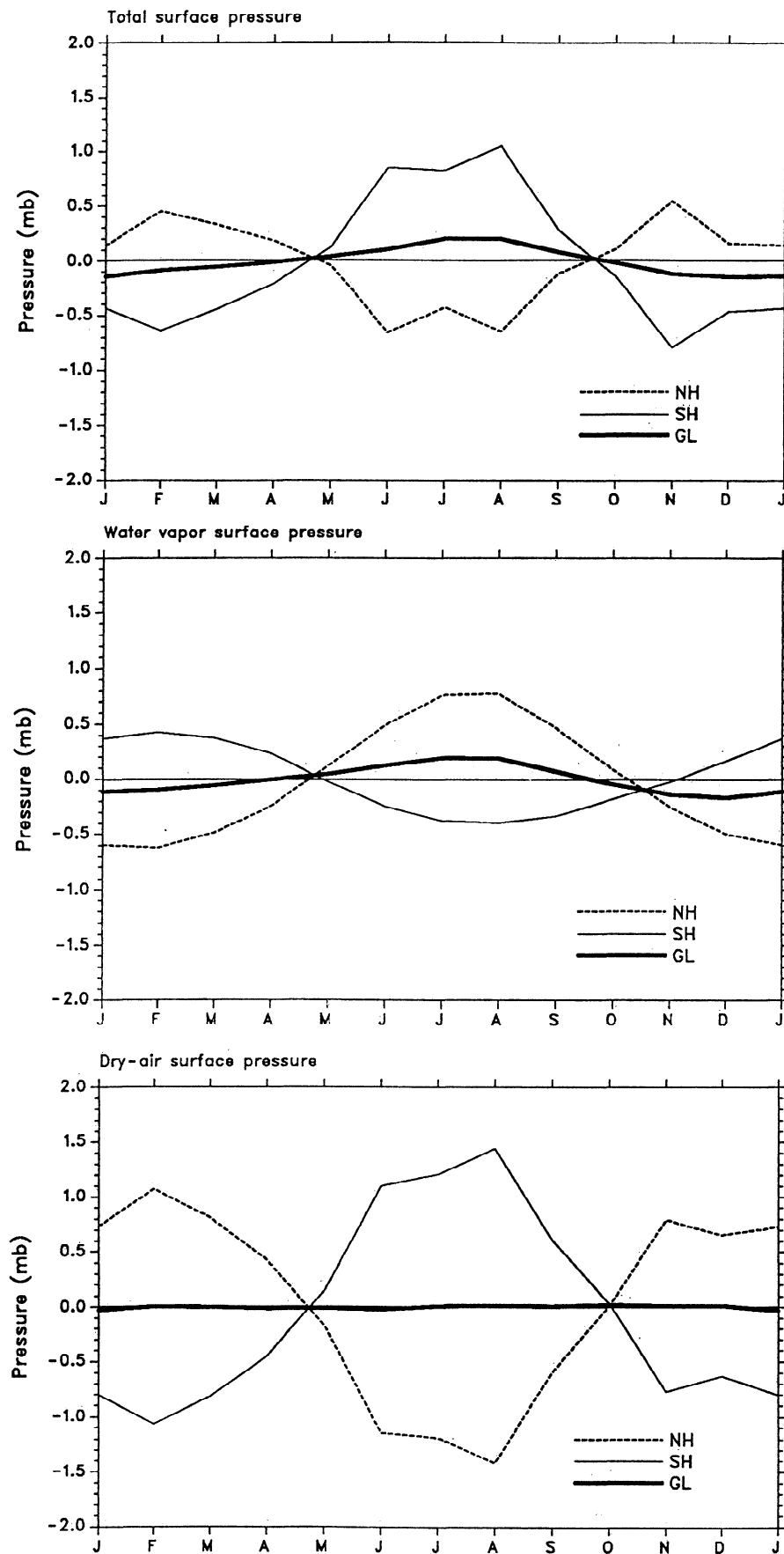


**Figure 2.** Mean annual cycle for 1985-1993 of (top)  $p_s$  and (middle)  $p_w$  and (bottom)  $p_d = p_s - p_w$ . Values are shown for the northern hemisphere (NH), southern hemisphere (SH), and the globe in mbar.

exceedingly small deviations from zero are a measure of the inaccuracies in the average data. Similar figures are shown by *Trenberth et al.* [1987] for the December 1978 to December 1985 period. A comparison shows that the annual cycle of  $p_w$  is quite stable, but there are noticeable changes in the hemispheric mean annual cycles for  $p_s$  and  $p_d$  that apparently arise from the interannual variability (see section 6).

The mean annual cycles as a function of latitude of  $p_s$  and  $p_w$  areally weighted by  $\cos \phi$ , so that the contribution to the global mean can be readily assessed, is shown in Figure 3. This reveals the large annual cycle associated with the tropical and subtropical monsoons with higher pressures in the subtropics of the winter hemisphere and an annual amplitude of about 2.5 mbar near 20°S and slightly less at 20°N. The migration of dry air seasonally across the equator corresponds to a vertical and zonal mean meridional velocity peaking at about  $1.5 \text{ mm s}^{-1}$  and flowing northward in August–September–October and southward in April–May–June [*Trenberth et al.*, 1987]. The flow of dry air across the equator is compensated by a summertime increase in moisture which has an annual

cycle with amplitude of 0.7 mbar in the NH and 0.5 mbar in the SH.

## 6. Interannual Variability

Interannual variations in the total atmospheric mass might be expected as the loading of water vapor increases, for instance, as part of the El Niño phenomenon [e.g., *Gaffen et al.*, 1991]. Similarly, upward trends in water vapor content are anticipated from model studies of “global warming” and climate change associated with increases in greenhouse gases in the atmosphere [*Intergovernmental Panel on Climate Change (IPCC)*, 1990, 1992]. Unfortunately, the observations of water vapor in the atmosphere are of poor quality and suffer from changes in instrumentation with time, that make detection of reliable trends difficult [*Trenberth et al.*, 1987; *Gaffen et al.*, 1991]. Similarly, global mean  $p_s$  suffers from lack of observations over vast areas and has been previously found to vary with a monthly standard deviation of 0.1 mbar relative to the long-term monthly means [*Trenberth et al.*,

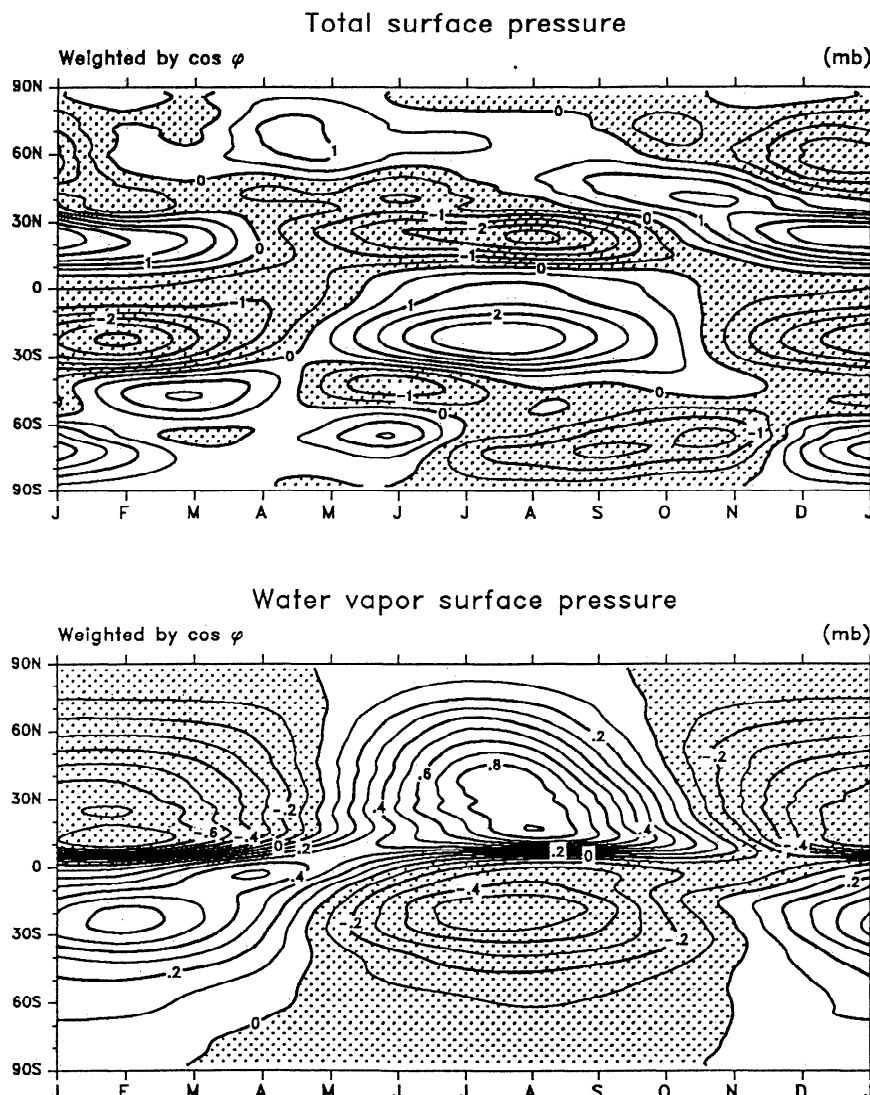


**Figure 3.** Mean annual cycle for 1985–1993 as a function of latitude of  $p_s \cos \phi$ , contour interval 0.5 mbar (top), and  $p_w \cos \phi$ , contour interval 0.1 mbar (bottom).

1987]. These variations were not reflected in similar global mean  $p_w$  variations, so it was concluded that this was an indication of the noise level in the data. The estimate of the signal from either El Niño or from decadal trends is about 0.05 mbar, which was masked in the previous study by the noise.

Nevertheless, it is of interest to see to what extent the global mean anomalies of  $p_s$  and  $p_w$  parallel one another for the recent period of record. Note that failure to find similar changes in these global mean quantities does not mean that there are not significant changes either locally in space or at certain levels in the vertical. On the contrary, *Gaffen et al.* [1991] do find regional evidence for climate change in the moisture field.

The time series of the hemispheric and global mean anomalies of  $p_s$ ,  $p_w$ , and  $p_d$  are shown in Figure 4. Large interannual variations are present in hemispheric mean  $p_s$ , but they are compensated for by opposite changes in the other hemisphere. This aspect has been pursued by *Trenberth and Christy* [1985] who analyzed the global modes of variability. In addition, *Trenberth* [1984] was able to confirm the existence of the exceptionally low pressures in the SH circumpolar trough for 1979 during the Global Weather Experiment using the constraint of conservation of mass. For the period shown in Figure 4, notable excursions in the hemispheric means occur. Early to mid-1990 and the northern winter of 1991–1992 are both examples of relatively high SH  $p_s$  and low NH  $p_s$  lasting over 4 months. The last eight months of 1993 are an example where positive anomalies persisted in the NH, with low values over the SH.

For the global mean anomalies in  $p_s$  and  $p_w$  in Figure 4 it is clear that the series are not stationary. However, as both are measures of the water vapor loading of the atmosphere, the only way to check on the reality of the trends is to also examine  $p_d$ . Here it is immediately obvious that something unphysical has produced a spurious trend as there is an apparent increase in the atmospheric mass of dry air with time. Alternatively, the two measures of precipitable water content of the atmosphere disagree. Thus broken into components, it can be seen that the trend arises from both increases in  $p_s$  and decreases in  $p_w$ . As we have found in the past [*Trenberth*, 1992], the trends are confounded by system changes in the analyses at ECMWF.

For this period, major impacts on these fields can be seen from changes on (1) May 1, 1985, when the T106 spectral model was introduced along with the hybrid vertical coordinate and major changes in the parameterizations of clouds and convection; (2) September 2, 1986, in which revisions were made in the use of observations, evaluation of increments, and data selection in analyses; and April 7, 1987, when surface parameterization schemes and postprocessed surface parameters were revised; (3) May 2, 1989, when there were substantial changes in model physics (radiation, mass flux cumulus parameterization, and gravity wave drag). (4) August 29, 1989, when analysis changes were made in aircraft and satellite data handling as well as the analysis first guess and low-level temperature increments; (5) September 17, 1991, when the T213 and 31 level analysis and forecasting system was implemented with a reduced Gaussian grid and changes to advection, horizontal and vertical diffusion, and clouds; (6) June 9, 1992, when humidity data from SYNOPs were excluded, and June 23, 1992, when the one-dimensional variational (1DVAR) analysis of cloud-cleared

satellite radiances were implemented.

The changes in May 1985, May 1989, and September 1991 were major model changes that had substantial impacts on the water vapor field. There were also changes in the topography and  $p_s$ , as analyzed by ECMWF at these times in 1985 and 1991, but they are not seen because of our recomputation of  $p_s$ . The trends in  $p_s$  seem to arise primarily from the changes in April 1987 and August 1989. We have examined global means for the  $p_s$  anomalies before, between and after these dates, but locally the natural variability dominates and there are no regions, such as mountain areas, that stand out. Instead, the effects are tiny but systematic over the entire globe. As shown by *Trenberth* [1992], it seems likely that the actual changes responsible for the  $p_s$  trends prior to 1992 were the switch from analyses in  $p$  coordinates to model coordinates in April 1987 and the improper use of single-level data prior to August 1989 [*Trenberth*, 1992, p. 38]. A substantial drop occurred in  $p_w$  in June 1992 and arose from the rejection of SYNOP humidity data which was done specifically “to reduce excessive convective precipitation in short and early medium-range forecasts,” to quote the September 1992 *ECMWF Newsletter*. While the implementation of the 1DVAR scheme directly impacts moisture through the TOVS water vapor channels, it was implemented only north of 20°N and thus is not the explanation (ECMWF, personal communication, 1994).

Because of the spurious changes in time, it is not clear from the above what the best value for the global mean  $p_w$  might be. As part of a separate project, we have compared ECMWF precipitable water with Special Sensor Microwave Imager (SSM/I) data from F. Wentz [see *Liu et al.*, 1992] for July 1987 to June 1991. The SSM/I data are available only over the oceans, and the annual mean over the global oceans for the 4-year period is 26.8 mm compared with 28.9 mm from ECMWF for the same region (and coincidentally compared with the global mean from ECMWF of 26.8 mm for the same period). Note that 1 mm is the same as 1 kg m<sup>-2</sup>. As found also by *Liu et al.* [1992], ECMWF values are too large in the subtropics and somewhat too low in the intertropical convergence zones. Full results will be reported on elsewhere. The implication is that overall there was a bias of ~2 mm in precipitable water over the oceans which converts to about 0.2 mbar in  $p_w$ . Accordingly, there is much less bias globally after June 1992, although regionally, substantial differences remain between the annual mean precipitable water from ECMWF in 1993 and the 4-year mean (July 1987 to June 1991) from SSM/I.

It is also of interest to examine the meridional profiles of the interannual variability because of the presence of two El Niño events (1986–1987 and 1991–1992) and a La Niña 1988–1989 during this period. Figure 5 shows the latitude-time sections with a  $\cos \phi$  area weighting applied. As we have seen previously [*Trenberth and Christy*, 1985; *Trenberth et al.*, 1987; *Christy et al.*, 1989], the dominant variation is one where mass exchanges occur between 30° to 60°S and south of 60°S and there is a similar but less active mode within the NH.

A signature of the El Niño events is an expectation of more precipitable water, with an increase in the tropical regions. The 1986–1987 event began around August 1986 and continued until January 1988 and does seem to be accompanied by a marked increase in  $p_w$  from 20°N to 25°S of 0.2 mbar (or 2 mm of precipitable water) in the zonal mean.

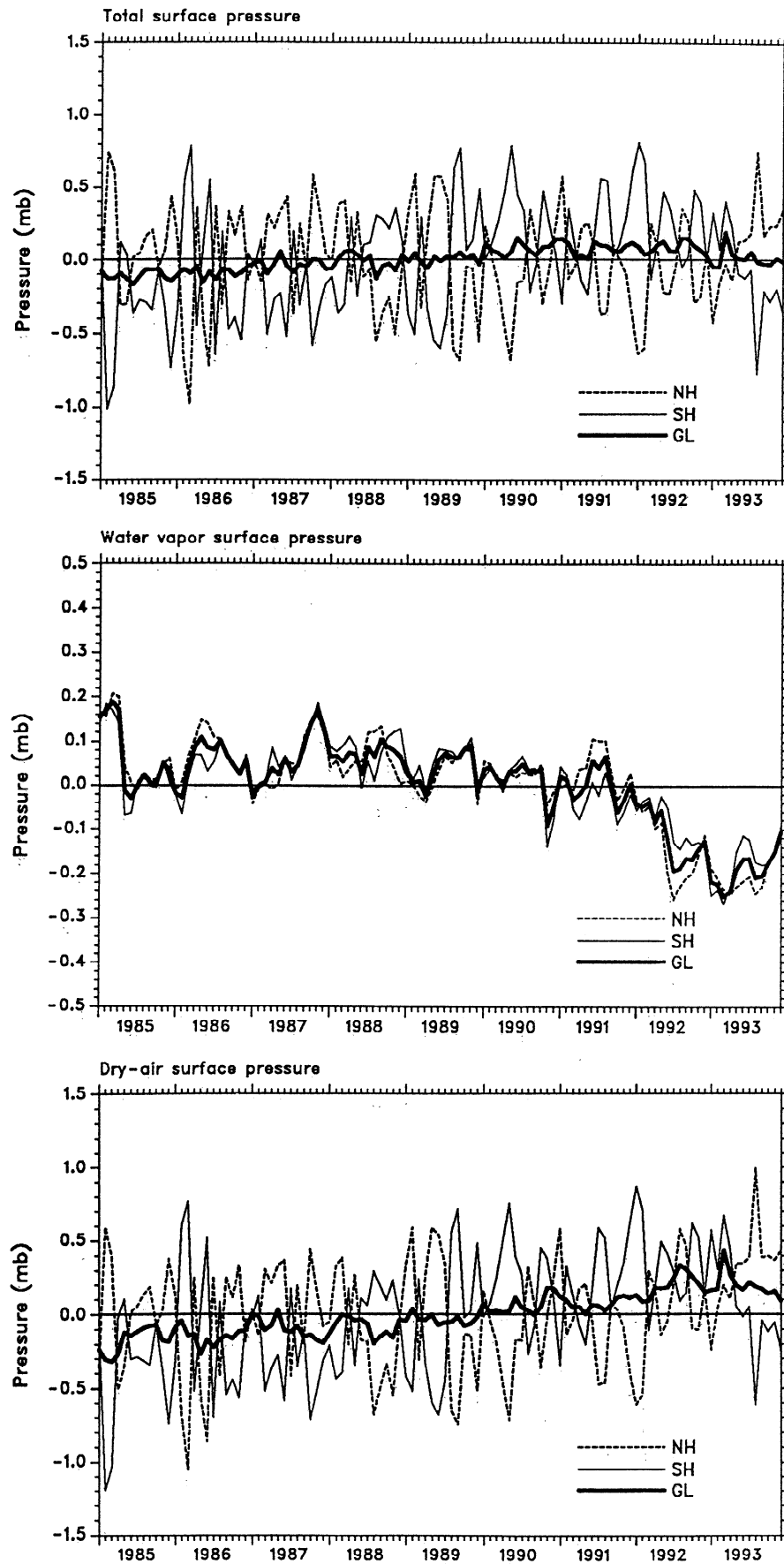


**Figure 4.** Anomalies (departures from mean annual cycle for 1985-1993) of (top)  $p_s$  and (middle)  $p_w$  and (bottom)  $p_d = p_s - p_w$ . Values are shown for the NH, SH, and the globe in mbar.



The 1991–1993 event began about April 1991, when a similar increase from 0 to 10°N occurs, but the changes are masked by the changes in the analysis system discussed earlier.

Another important factor may have been the eruption of Mount Pinatubo on June 15, 1991, which deposited a veil of aerosol in the stratosphere and was forecast to reduce global temperatures by about 0.5°C by Hansen *et al.* [1992] and has evidently done so (Figure 1.5 of U.S. Department of Commerce, 1994). The global cooling in the last 7 months of 1992, in particular, could have substantially impacted the moisture content of the atmosphere. However, a check of the changes in temperatures and relative humidities shows that the change is mainly in the latter. The moisture decrease is seen in the tropics (Figure 5), while the surface temperature decrease was mostly in the NH extratropics. Hence, overall, there is not a good match between the moisture and the temperature changes, either in time or as a function of latitude, and the evidence suggests that the changes in analysis procedures overwhelm any climate signal. A reanalysis of the data will facilitate study of these intriguing interannual variations.

## 7. Conclusions

Accurate formulae for determining the mass of the atmosphere in terms of the surface pressure  $p_s$  have been derived and applied to ECMWF data for 1985 through 1993. The formulae factor in effects on the shape of the Earth and variations in gravity with latitude and height. Variations in total mass occur because of changes in the water vapor loading of the atmosphere. Spurious trends in both the mass of dry air and the atmospheric moisture are found to arise from changes in the analysis system at ECMWF.

In view of the spurious trends in both  $p_s$  and  $p_w$  arising from improvements in the system, it seems that the best estimate of the total mass of the atmosphere should be one based on the more recent analyses. For the 4-year period 1990 to 1993 the mean annual  $p_s$  was reasonably stable at 984.76 mbar with a maximum in July of 984.98 mbar and a minimum in December of 984.61 mbar. Thus the total mass of the atmosphere is  $5.1441 \times 10^{18}$  kg with a range of  $1.93 \times 10^{15}$  kg throughout the year associated with changes in water vapor in the atmosphere. There is excellent agreement

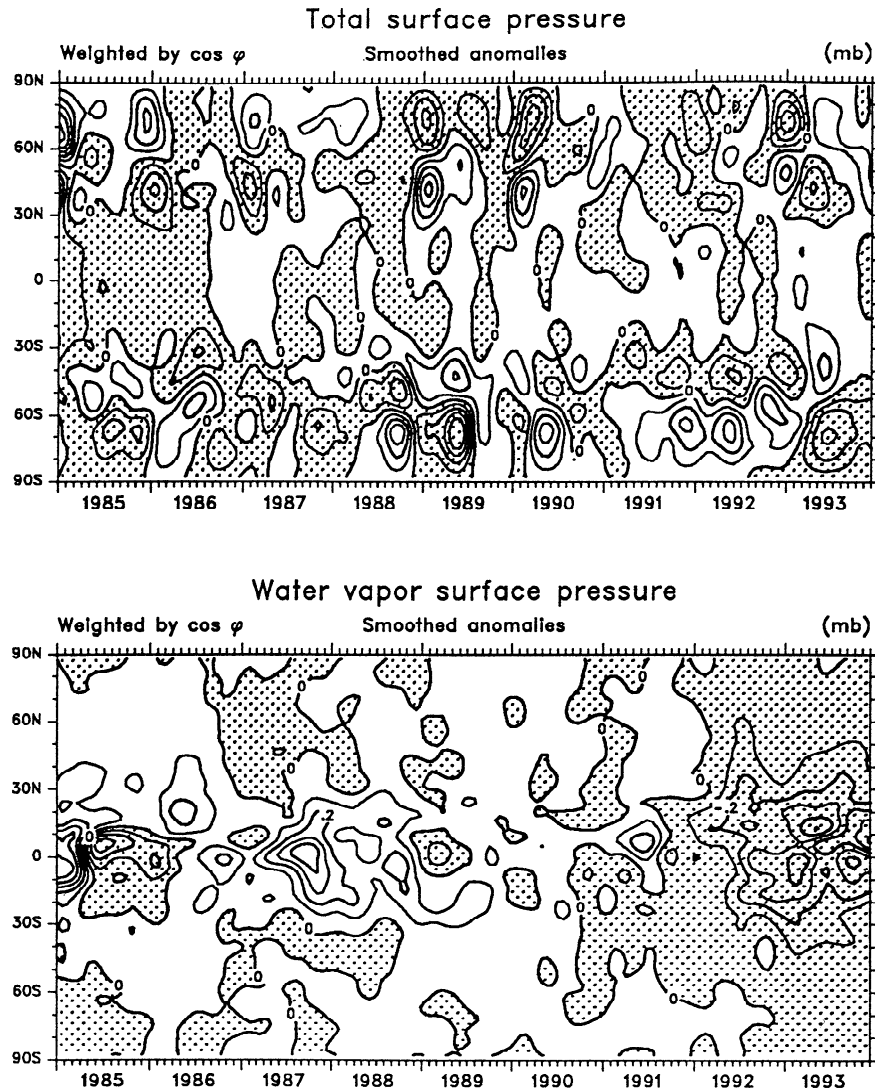


**Figure 5.** Anomalies as a function of latitude of (top)  $p_s \cos \phi$  and (bottom)  $p_w \cos \phi$  in mbar. Contour interval is (top) 0.5 mbar and (bottom) 0.1 mbar.

between the mean annual cycles from  $p_s$  and  $p_w$ , and the global mean  $p_w$  varies by 0.36 mbar with an annual cycle maximum in July and a minimum in December.

The global mean water vapor surface pressure  $p_w$  varies in a spurious way along with changes in the ECMWF analysis system by  $\sim 0.2$  mb (Figure 4), and similar changes have been seen in previous years [Trenberth *et al.*, 1987]. The mean of the entire period for this quantity for 1985–1993 is 2.58 mbar corresponding to 2.63 cm of precipitable water. But after mid-1992, mean values are 2.4 mbar and thus close to 1-in. of precipitable water. The mean mass of water vapor for 1985–1993 is  $1.35 \times 10^{16}$  kg, but as discussed in section 6, a more realistic value is probably that following the changes in mid-1992 of  $1.25 \times 10^{16}$  kg. Hence the dry air mass is  $5.132 \times 10^{18}$  kg, corresponding to a mean surface pressure of 982.4 mbar. As seen above, the uncertainties are about 0.1 mbar or  $0.5 \times 10^{15}$  kg in  $p_s$  and about double those values for  $p_w$  and  $p_d$ . The mean annual cycle is known much more accurately; it is the annual average water content that has greatest uncertainty. The differences from previous values of Trenberth [1981] in the revised numbers are within this uncertainty.

Differences from previous estimates arise from (1) modifications in the methodology as detailed in section 3 leading to the development of equation (13), which produces a slight increase, and (2) the new global data at higher spatial resolution and 4 times daily plus more information in the vertical as well as improved procedures for producing the global analyses. Some uncertainties remain in these numbers and it is not yet possible to obtain reliable estimates of the interannual or interdecadal variability of the total mass which arise through changes in water vapor loading.

**Acknowledgments.** We thank Dave Fultz for bringing the historical papers to our attention. This research is partially sponsored by the Tropical Oceans Global Atmosphere Project Office under grant NA87AANRG0208. The data used were provided by ECMWF. The National Center for Atmospheric Research is sponsored by the National Science Foundation.

## References

- Abbe, C., The weight or mass of the atmosphere. *Mon. Weather Rev.*, 27, 58–59, 1899.
- Bernhardt, K., Bodenluftdruck, Masse und potentielle Energie der Atmosphäre im Schwerefeld, *Meteorol. Z.*, 41, 18–24, 1991a.
- Bernhardt, K., Globale Erwärmung und Änderung des mittleren Luftdruckes an der Erdoberfläche, *Meteorol. Z.*, 41, 325–332, 1991b.
- Buchan, A., The mean pressure of the atmosphere and the prevailing winds over the globe, *Trans. R. Soc. Edinburgh*, 25, 575–637, 1869.
- Christy, J. R., K. E. Trenberth, and J. R. Anderson, Large-scale redistributions of atmospheric mass, *J. Clim.*, 2, 137–148, 1989.
- Ekholm, N., Über die Höhe der homogenen Atmosphäre und die Masse der Atmosphäre, *Meteorol. Z.*, 19, 249–260, 1902.
- Ferrel, W., *Meteorological Researches for the Use of the Coast Pilot*, U.S. Government Printing Office, Washington, D. C., 1877.
- Gaffen D. J., T. P. Barnett, and W. P. Elliott, Space and time scales of global tropospheric moisture, *J. Clim.*, 4, 989–1008, 1991.
- Hansen, J., A. Lacis, R. Ruedy, and M. Sato, Potential climate impact of Mount Pinatubo eruption, *Geophys. Res. Lett.*, 19, 215–218, 1992.
- Intergovernmental Panel on Climate Change (IPCC), *Scientific Assessment of Climate Change*, edited by J. T. Houghton, G. J. Jenkins, and J. J. Ephraums, 365 pp., Cambridge University Press, New York, 1990.
- IPCC, *Climate Change 1992*, edited by J. T. Houghton, B. A. Callander, and S. K. Varney, 200 pp., Cambridge University Press, New York, 1992.
- Letestu, S., WMO international tables, *WMO, 188 TP94*, World Meteorol. Organ., Geneva, 1966.
- Liu, W. T., W. Tang and F. Wentz, Precipitable water and surface humidity over global oceans from Special Sensor Microwave Imager and European Centre for Medium-Range Weather Forecasts. *J. Geophys. Res.*, 97, 2251–2264, 1992.
- Pascal, B., Traite de la pesanteur de la masse de l'aire, pp. 193–253; Combien pese la masse entiere de tout l'aire que' est au monde, pp. 248–253, in *Grands Ecrivains de la France*, 1663.
- Trenberth, K. E., Seasonal variations in global sea level pressure and the total mass of the atmosphere, *J. Geophys. Res.*, 86, 5238–5246, 1981.
- Trenberth, K. E., Interannual variability of the Southern Hemisphere circulation: Representativeness of the year of the Global Weather Experiment, *Mon. Weather Rev.*, 112, 108–123, 1984.
- Trenberth, K. E., Global analyses from ECMWF and atlas of 1000 to 10 mb circulation statistics, *NCAR Tech. Note, NCAR/TN-373+STR*, 191 pp. plus 24 fiche, Nat. Cent. for Atmos. Res., Boulder, Colo., 1992.
- Trenberth, K. E., and J. R. Christy, Global fluctuations in the distribution of atmospheric mass, *J. Geophys. Res.*, 90, 8042–8052, 1985.
- Trenberth, K. E., and J. G. Olson, An evaluation and intercomparison of global analyses from NMC and ECMWF, *Bull. Am. Meteorol. Soc.*, 69, 1047–1057, 1988.
- Trenberth, K. E., J. R. Christy and J. G. Olson, Global atmospheric mass, surface pressure, and water vapor variations, *J. Geophys. Res.*, 92, 14,815–14,826, 1987.
- U.S. Department of Commerce, *Fifth Annual Climate Assessment 1993*, Climate Analysis Center, National Oceanic and Atmospheric Administration, Washington, D. C., 1994.
- C. J. Guillemot and K. E. Trenberth, National Center for Atmospheric Research, P.O. Box 3000, Boulder, CO 80307. (e-mail: chrisg@ncar.ucar.edu, trenbert@ncar.ucar.edu)

(Received March 30, 1994; revised August 8, 1994; accepted August 8, 1994)